



Open Access

ORIGINAL ARTICLE

Sperm Biology

Anatase titanium dioxide nanoparticles in mice: evidence for induced structural and functional sperm defects after short-, but not long-, term exposure

Michelle A Smith¹, Rowan Michael¹, Rolands G Aravindan¹, Soma Dash¹, Syed I Shah², Deni S Galileo¹, Patricia A Martin-DeLeon¹

Titanium dioxide (TiO₂) nanoparticles (TNPs) are widely used commercially and exist in a variety of products. To determine if anatase TNPs (ATNPs) in doses smaller than previously used reach the scrotum after entry in the body at a distant location and induce sperm defects, 100% ATNP (2.5 or 5 mg kg⁻¹ body weight) was administered intraperitoneally to adult males for three consecutive days, followed by sacrifice 1, 2, 3, or 5 weeks later (long-) or 24, 48 or 120 h (short-term exposure). Transmission electron microscopy revealed the presence of ANTP in scrotal adipose tissues collected 120 h postinjection when cytokine evaluation showed an inflammatory response in epididymal tissues and fluid. At 120 h and up to 3 weeks postinjection, testicular histology revealed enlarged interstitial spaces. Significantly increased numbers of terminal deoxyribonucleotidyl transferase-mediated dUTP nick-end labeling-positive (apoptotic) germ ($P = 0.002$) and interstitial space cells ($P = 0.04$) were detected in treated males. Caudal epididymal sperm from the short-term, but not a long-term, arm showed significantly ($P < 0.001$) increased frequencies of flagellar abnormalities, excess residual cytoplasm (ERC), and unreacted acrosomes in treated versus controls (dose-response relationship). A novel correlation between ERC and unreacted acrosomes was uncovered. At 120 h, there were significant decreases in hyperactivated motility ($P < 0.001$) and mitochondrial membrane potential ($P < 0.05$), and increased reactive oxygen species levels ($P < 0.00001$) in treated versus control sperm. These results indicate that at 4–8 days postinjection, ANTP induce structural and functional sperm defects associated with infertility, and DNA damage via oxidative stress. Sperm defects were transient as they were not detected 10 days to 5 weeks postinjection.

Asian Journal of Andrology (2015) 17, 261–268; doi: 10.4103/1008-682X.143247; published online: 24 October 2014

Keywords: cytoplasmic droplets; oxidative stress; sperm motility defects; unreacted acrosomes

INTRODUCTION

Titanium dioxide (TiO₂) nanoparticles (TNPs) are commonly used in consumer products such as cosmetics and medicines¹ and in photocatalytic applications for environment remediation^{2,3} where they are difficult to remove after water treatment.⁴ Thus, it is important to fully assess the biological effects of exposure to these nanoparticles. To date, only few studies have investigated their effects on the reproductive system which is known to be sensitive to both carbonaceous particles, and metal-based nanoparticles.^{5–7} Recent reviews^{5–7} have highlighted the limited knowledge that exists regarding reproductive toxicological effects of TNP and have suggested “the relevance of the topic makes future investigations a matter of urgency.”⁶ Although there are several forms of TNP, rutile and anatase TNP (ATNP) are the main polymorphs that are manufactured commercially and the latter has been shown to have a higher photocatalytic activity than the rutile form.⁸

The high reactivity of ATNP is seen in their production of reactive oxygen species (ROS) in aqueous systems,^{8,9} and exposed cells have revealed evidence of this.^{10,11} Furthermore in the absence of light, ATNP systems can generate radical species in cultured human dermal

fibroblasts and lung epithelial cells under a range of conditions.⁸ Furthermore, the quantity of ROS is increased in culture medium, and there is an additional increase in the presence of ultraviolet light.⁸ Importantly, *ex vivo* ROS generation from TNP correlated with biological responses that included membrane damage. Overall, there appears to be enough evidence to implicate NP/ATNP surfaces in oxidative damage of biological material even in the absence of light.^{5–8,12}

In mice, detrimental effects were observed in the offspring of treated females after prenatal exposure: at a total dosage of 400 µg (in four injections), ATNP administered subcutaneously over an 11 days period postcoitum resulted in damage to the cranial and genital system in male offspring at postnatal day 4 and postnatal week 6.^{7,13} In this offspring ATNP were detected in Leydig cells, spermatids and Sertoli cells, and the seminiferous tubules appeared disorganized.¹³ Interestingly, *in vitro* study showed uptake of TNP in mouse Leydig cells with an effect on viability, proliferation and gene expression,¹⁴ although TNP is less cytotoxic than AgNP in these cells.¹⁵ To date, two studies have investigated the effects of TNP on the adult male reproductive tract: sexually mature mice were administered high doses of TNP via

¹Department of Biological Sciences, University of Delaware, Newark, DE, USA; ²Departments of Physics and Astronomy and of Material Science, Engineering, University of Delaware, Newark, DE, USA.

Correspondence: Prof. PA Martin-DeLeon (pdeleon@udel.edu)

Received: 08 April 2014; Revised: 10 June 2014; Accepted: 27 June 2014

intraperitoneal injections (200–500 mg kg⁻¹ body weight [BW])¹⁶ or oral gavage (40–1000 mg kg⁻¹ BW)¹² and showed decreases in sperm count and motility and induced germ cell apoptosis,¹⁶ along with increased frequency of spermatids with 2 or more nuclei.¹²

The present study was performed to examine the effects of ATNP in adult mice, using lower dosages (>200 times lower) than previously administered intraperitoneally, to determine if ATNP bioaccumulate in the scrotum and impact sperm after long- or short-term exposure. Long-term exposures were selected to include a timeline for the completion of spermatogenesis (>35 days¹⁷) postadministration while short-term exposures occurred during the ~5–10 days required for epididymal sperm maturation.¹⁸ Our results show that these smaller ATNP doses travel from the peritoneal cavity to the scrotum where they aggregate, impact testicular histology, and adversely affect sperm structurally and functionally 4–8 days, but not 10–38 days, postinjection. Motility defects were associated with increases in ROS, suggesting that oxidative stress may be the underlying mechanism for the induction of the abnormalities.

MATERIALS AND METHODS

Animals and reagents

Sexually mature 3–6 months old male outbred mice (ICR and C57BL/6 strains; Harlan, Indianapolis, IN, USA) were randomly chosen for the investigation. Studies were approved by the Institutional Animal Care/Use Committee at the University of Delaware. Chemicals were purchased from Fisher Scientific (Malvern, PA, UK), Sigma-Aldrich (St. Louis, MO, USA) or Invitrogen (Carlsbad, CA, USA), unless otherwise specified.

Anatase titanium dioxide nanoparticles preparation

Anatase TNPs were synthesized by a chemical vapor deposition process (CVD), using titanium tetrakispropoxide (TTIP), 97% purity, as a precursor with oxygen and argon gases as oxidizer and carrier gases. Details of this synthesis have been previously described.¹⁹ Briefly, the CVD system is a hot wall system comprised of stainless steel tube reactor which was maintained at 600°C. A mechanical pump was used to pump the reaction chamber down to a few millitorr base pressure. The liquid TTIP was placed in a heated round bottom flask; 99.999% pure Ar (Keen Gas) was used as the carrier gas by bubbling it through the TTIP. The precursor flow rate was adjusted by changing the flow rate of Ar through the bubbling chamber. O₂ was added to the Ar/TTIP mixture in the reactor chamber for the TiO₂ formation. TNP was collected on several layers of 400 mesh stainless steel screens, to increase collection efficiency. Samples were analyzed by X-ray diffraction and show typical anatase diffraction pattern. No rutile related diffraction peaks were observed. The particle size of the ATNP was 50 ± 8 nm.

Dosage concentrations and injections

Males (~25 g) were randomly selected and injected intraperitoneally with 0.1 ml of phosphate buffer saline (PBS) (vehicle control) or 0.1 ml PBS containing 62.5 µg (low) or 125 µg (high) of 100% ATNP suspended in the solution without sonication. Injections were given at the same time daily for three consecutive days, with the working solution freshly made from stock. Dosages were 2.5 and 5 mg kg⁻¹ BW.

Study design and tissue recovery

For the long-term arm, a total of 36 mice were used in four groups of nine. Each group consisted of 3 males injected with PBS, 3 with the low, and 3 with the high ATNP dose. One of the four groups of nine was sacrificed on 1, 2, 3 or 5 weeks after the third injection. For the short-term arm, males were sacrificed after 24, 48 or 120 h

postinjections. For this arm 30 mice were used to study the dosage effect on sperm morphology, progressive motility, and the acrosome reaction (AR): 10 control mice, 9 exposed to the low and 11 to the high ATNP dose. Additionally, 22 mice (totaling 52 in the short-term arm) were used to study the effect of the high dose on hyperactivated motility (7), ROS levels (7), and apoptosis/mitochondrial membrane potential (MMP) (8/6) after 120 h. Thus a grand total of 88 mice were used in the study, 85 of which were of ICR, and 3 of C57BL/6J, strain. The three C57BL/6 males were in the short-term arm: 1 in the 10 control and 2 in the high exposure 120 h group where there were a total of 11. No strain differences were detected in the response to ATNP.

Mice were sacrificed (CO₂ asphyxiation) and scrotal tissue examined before removal. Scrotal adipose tissue of a male in the 120 h group revealed white spicules. The tissue was removed for sectioning and analysis, using transmission electron microscopy (TEM). Testes were weighed and immediately fixed in 10% Bouin's solution or 4% paraformaldehyde (frozen sections) for histological analysis. Sections for light microscopy were routinely prepared and stained in hematoxylin and eosin (H and E). Terminal deoxyribonucleotidyl transferase-mediated dUTP nick-end labeling (TUNEL) assays were performed on frozen sections, routinely prepared, with the ApopTag Fluorescein *In Situ* Apoptosis Detection Kit (catalog no. S7110, Millipore, USA).

Transmission electron microscopy

Testes and scrotal adipose tissues were placed in fixative (2% glutaraldehyde and 2% paraformaldehyde in 0.1 mol l⁻¹ sodium cacodylate buffer), cut into small pieces, and held at 4°C until further processing. The fixed tissues were subjected to a series of washes consisting of 0.1 mol l⁻¹ sodium cacodylate buffer, osmium tetroxide, double deionized water and EtOH in which it was allowed to sit overnight at 4°C. They were infiltrated with a series of washes consisting of Embed-812 resin (with and without DMP-30 component) and 100% EtOH and allowed to sit overnight. The tissues were then infiltrated with fresh resin which was set into BEEM capsules and allowed to polymerize for 48 h at 70°C. Sections of tissues in polymerized resin were analyzed via TEM for the presence/absence of ATNP. To assist in the identification of the ATNP in sections, the stock solution of the ATNP used for injections was also subjected to TEM analysis.

Recovery of serum and epididymal tissues for cytokine evaluation

Approximately 400 µl of blood was collected and pooled from each of 4 treated (high dose) and 4 control males at 120 h postinjection via orbital bleeding, and serum recovered. Epididymal luminal fluids (ELF) and tissues were collected from all epididymal regions and tissue lysates prepared as described.²⁰ Serum diluted (5-fold) and 500 µg of total protein from ELF and tissue lysate were hybridized to a glass chip G-series inflammatory antibody array (RayBiotech, Norcross, GA, USA) according to manufacturer's guidelines. Fluorescence intensity was analyzed using a microarray scanner and software used to calculate the mean intensity of each spot minus background.

Sperm recovery, analysis of motility (progressive and hyperactivated) and structural defects

Caudal epididymides were removed and placed in 1 ml of human tubal fluid (HTE, with HEPES [InVitroCare, Frederick, MD, USA]) warmed to 37°C. Minced caudae were left for 10 min to allow sperm to swim out. The sperm suspension was aspirated for further processing. An aliquot was diluted and assessed (blindly) for progressive motility and morphology, using a hemacytometer, with ≥ 200 sperm per sample. Of the motile sperm counted, ~50 in each quadrant of the hemacytometer

were analyzed to detect excess residual cytoplasm (ERC) or cytoplasmic droplets, noting their sizes and locations.

To assess hyperactivated motility, sperm collected at 120 h were incubated under capacitating conditions (HTF medium) for 90 min at 37°C. An aliquot was then diluted 1:100 with prewarmed HTF and placed on a slide prewarmed to 37°C. Motility was determined after microscopic examination (blindly) for ~ 200 sperm per sample. To assess sperm morphology following incubation under capacitating conditions, an aliquot of the sperm suspension was fixed (4% paraformaldehyde) mounted on slides and stained with Coomassie Brilliant Blue.²¹ Sperm (≥ 200 sperm per sample) were analyzed blindly for morphological abnormalities.

Hyaluronic acid-enhanced progesterone-induced acrosome reactions

Acrosome reaction was induced under physiological conditions as previously described.²² Briefly, samples of $\sim 2.5 \times 10^5$ sperm in HTF were incubated at 37°C for 45 min, and treated with 100 $\mu\text{g ml}^{-1}$ hyaluronic acid for 30 min followed by progesterone (PG, 3.18 $\mu\text{mol l}^{-1}$ for 5 min). Sperm were then pelleted (500 g, 15 min) and re-suspended in 4% paraformaldehyde at room temperature overnight. A 1:5 dilution of the sperm suspension was prepared with PBS and 20 μl smeared on a slide, dried and stained with Coomassie Blue and then examined microscopically (blindly) to determine the percentage of acrosome-reacted sperm and those with ERCs in ≥ 200 , from three slides per animal.

Detection of reactive oxygen species and mitotracker staining in sperm collected at 120 h postinjection

To investigate the mechanism by which reduced motility was induced, a ROS detection kit (Cell Tech, Inc., Mountain View, CA, USA) measuring diverse species was used to determine ROS levels. Briefly, aliquots (3×10^6 – 5×10^6) of freshly recovered caudal sperm in PBS at 37°C were loaded with the hydroxyphenyl fluorescein probe diluted 1:130²³ and incubated at 37°C in the dark for 45 min. Cells were then placed in HTF medium and incubated at 37°C for 90 min after which PBS was added and 5×10^4 cells analyzed on the flow cytometer: excitation at 488 nm and emission at 515 nm. MMP was measured as previously described.²⁴ Briefly, aliquots of capacitated sperm were washed in PBS and incubated in a prewarmed PBS solution containing 250 nmol l^{-1} MitoTracker Red CMXRos, at 37°C for 30 min. They were then washed twice in PBS and subjected to flow cytometric analysis: excitation 532 nm, emission 600–620 nm.

Statistical analysis

Data were processed using Student's *t*-test and chi-squared (χ^2) analysis with Yates' correction. To determine a correlation between the sperm's inability to acrosome-react and ERC's presence, the Cochran–Mantel–Haenszel analysis for repeated tests of independence with continuity correction was used.

RESULTS

Transmission electron microscopy reveals that anatase titanium dioxide nanoparticles aggregate and bioaccumulate in scrotal tissue with resulting inflammation

There were no significant differences in the average testis weights (0.08–0.13 g) for treated and control groups. TEM revealed the crude, physical appearance of the ATNP (Figure 1a) and facilitated their identification in scrotal adipose tissues. While no particles were detected in the testis sections, TEM of adipose tissue sections containing the white spicule revealed aggregates of ATNP (Figure 1b), comparable to those detected in the ATNP solution that was injected (Figure 1a).

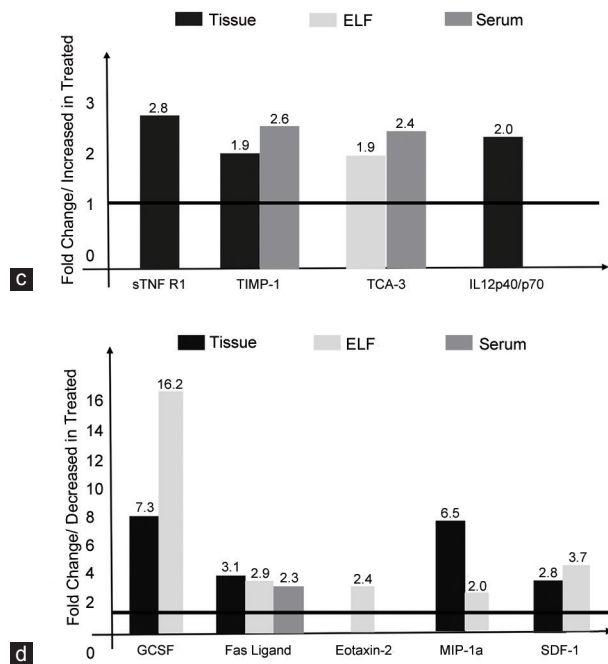
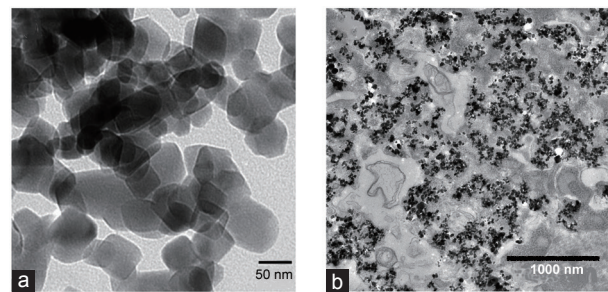


Figure 1: Anatase titanium dioxide (TiO_2) nanoparticles (ATNP) bioaccumulate in scrotal tissues with a resulting inflammatory cytokine response. (a) Transmission electron microscopy (TEM) image of ATNP in suspension seen at high magnification, scale bar = 50 nm. (b) TEM revealed ATNP aggregates, black dots, in adipose and connective tissues in the scrotum of a mouse exposed to a total of 375 $\mu\text{g TiO}_2$ and sacrificed 120 h postinjection, scale bar = 1000 nm. (c and d) A microarray panel of 40 classical cytokines was evaluated and the most striking differences between treated and controls are presented as fold change for (c) increased and (d) decreased levels of expression in the treated group for individual cytokines. The lines parallel to the X-axis show the control (c) and treated levels (d).

The spicule was visually identified in the adipose tissues surrounding the testis and epididymis of a mouse exposed to the high dosage of ATNP 120 h postinjection. This TEM finding indicates that ATNP are transported from the peritoneal cavity to the scrotum where they bioaccumulate or aggregate around testicular and epididymal tissues. Evidence of ANTP's presence in the scrotum is seen by changes in the epididymal inflammatory status at 120 h postinjection. The most striking differences in the cytokine profile for serum, epididymal tissues and ELF for treated and controls are seen in Figure 1c and 1d. Fold change increases ranged from 1.9 to 2.8 for 4 cytokines (Figure 1c) and decreases from 2.3 to 16.2 for 5 (Figure 1d).

Histological analysis revealed testicular abnormalities after exposure to anatase titanium dioxide nanoparticles

Hematoxylin and eosin stained testis sections revealed interstitial spaces which, compared to controls (Figure 2a), were enlarged after treatment with both dosages (Figure 2b and 2c). Males sacrificed

at 120 h postinjection showed the effects with the high dosage, while with long-term exposure (weeks 1–3) they were seen with both dosages. Additionally, the seminiferous tubules in the treated groups, when compared to controls, had large spaces devoid of germ cells and appeared disorganized (**Figure 2b** and **2c**); while the TUNEL assay (**Figure 2d–2j**) showed significantly increased numbers of apoptotic germ ($P = 0.002$, $P = 0.04$) and interstitial space cells ($P = 0.04$).

Analysis after long-term exposure: sperm are unaltered structurally and functionally

Microscopic analysis revealed similar percentages (17%–30%) of sperm with ERC in each of the 4 weeks where > 1800 sperm were analyzed in the two dosage and the control groups from 9 males. Thus there was no significant differences between the controls and treated in the 36 males tested. Similarly, the percentages (30%–50%) of motile sperm in each of weeks 1, 2, 3, and 5 postinjection showed no significant

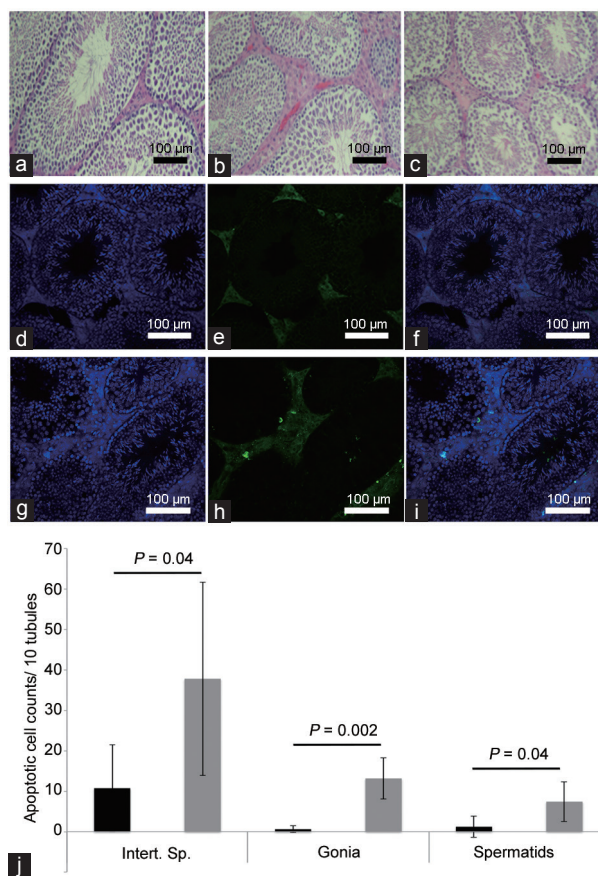


Figure 2: Altered testis histology (H and E staining) and increased apoptotic germ and interstitial space cells follow anatase titanium dioxide nanoparticles exposure. In (a) normal seminiferous tubules and interstitial spaces are seen in the control; while (b and c) show sections, from the low and high dose, with enlarged interstitial spaces and tubules that are disorganized to different degrees. Scale bar = 100 μ m. Terminal deoxyribonucleotidyl transferase-mediated dUTP nick-end labelling (TUNEL)-positive cells in testis from control (d–f) and treated (g–i) males (high dose after 120 h) where the yellow signal is bright in an enlarged interstitial space and in spermatogonia. (j) Distribution of apoptotic cells from the TUNEL assay with 140 and 147 tubules and the surrounding interstitial spaces analyzed for each of the 4 control and treated animals. Interst. Sp.: cells in the interstitial spaces; Gonia: spermatogonia. A Student's *t*-test shows significant differences ($P < 0.05$ taken as significant) between control and treated for all cell types, with the difference being highly significant ($P = 0.002$) for spermatogonia. Error bars are standard deviations.

differences between control and test groups. We then tested the ability of sperm to acrosome-react after exposure. Acrosome-unreacted and -reacted-sperm were identified by the presence (**Figure 3a**) or absence (**Figure 3b**) of a stained (blue) acrosomal cap. No significant differences in the rate of AR were detected for the low (42%–51%) or high (49%–50%) doses versus controls (46%–47%) for the periods studied (weeks 1, 3, and 5).

Acrosome reaction and motility rates are significantly reduced after short-term exposure

An unbiased analysis of sperm (**Figure 3a** and **3b**) on coded slides revealed that the rates of AR induced physiologically were highest in the controls (41.7%, 69.5%, and 55.9%) for the three short-term periods (**Table 1a**) and similar to those in the long-term arm (42%–51%). However, AR rates were 30.6%–54.8%, for the low and 29.7%–36.6% for the high dosages (**Table 1a**). Chi-squared analysis revealed a highly significant ($P < 0.001$) difference between total controls and treated groups. Importantly, 3×2 contingency tables showed there was a significant relationship between the rate of AR and dosage for the grand total ($\chi^2 = 164.93$, $P < 0.0001$), the 48 h ($\chi^2 = 15.86$, $P < 0.0001$), and 120 h ($\chi^2 = 53.39$, $P < 0.0001$), but not the 24 h group ($\chi^2 = 0.52$, $P = 0.4708$), indicating that length of exposure

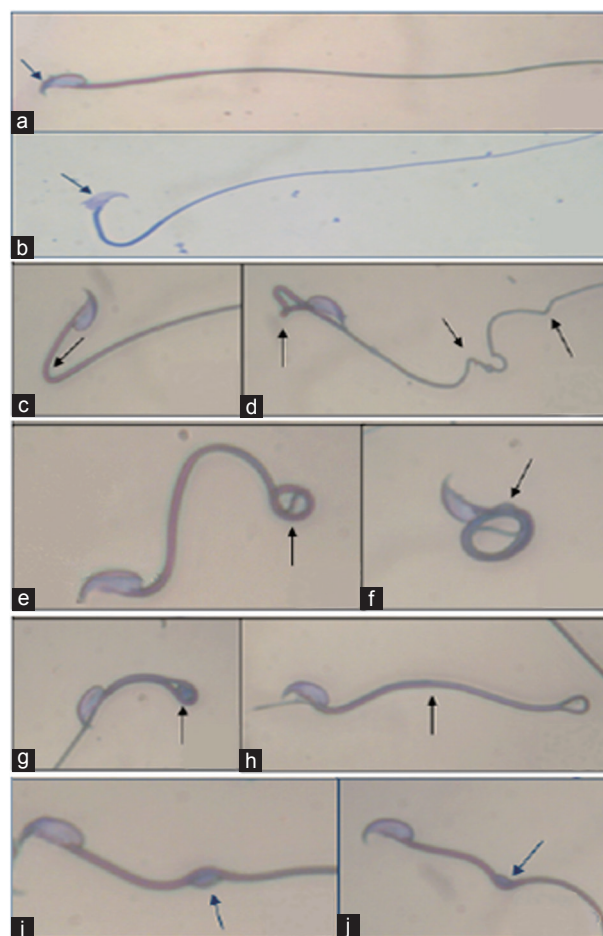


Figure 3: The detection of acrosomal status and tail abnormalities via Coomassie Blue staining after anatase titanium dioxide nanoparticles exposure. (a) A sperm with an intact acrosomal cap (arrowed), while (b) the cap missing after AR. Arrows indicate kinks (c and d), coils (e and f), and folds (g and h). Excess residual cytoplasm (arrowed) are present in concave curvatures near the midpiece (g and j) and in a convex curvature (i).

is a factor in the disruption of the sperm's ability to acrosome-react after treatment.

Progressive motility rates (**Table 1b**) showed a significant ($P < 0.001$) decline between the control and the low, but not the high, dose at 24 h. At 48 h there was a significant ($P < 0.001$) decline between the controls and the high, but not the low, dose. Although at 120 h both treated groups has reduced motility compared to the controls, with the rate for the high dose being lower than that for the low, there was no significant difference between the groups (**Table 1b**). Consequently, we studied hyperactivated motility at 120 h for the high dosage and control groups. The latter showed a mean percentage rate of 46.1% (39.5%–52%) in contrast to 15.8% (14.1%–18.4%), for the treated group. The difference between these frequencies is highly significant ($\chi^2 = 285.2$; $P < 0.001$).

Structural sperm defects significantly increased after short-term exposure

Structural abnormalities detected included flagellar kinks (**Figure 3c** and **3d**), coiled (**Figure 3e** and **3f**) and folded tails (**Figure 3g** and **3h**) which often contained ERCs in different positions (**Figure 3g**, **3i** and **3j**). The frequencies of ERCs, the most common abnormalities, are presented in **Table 2a**; while the others showed ~ 3-fold increases in the treated groups (71.8% and 83.4%) for the low and high doses versus control (24.6%) at 120 h. A contingency table showed that there was a significant relationship between dosage and frequency ($\chi^2 = 57.31$, $P < 0.0001$). Slides with the data at 24 h and 48 h were only partially analyzable.

Excess residual cytoplasm (**Table 2a**) were observed in the same plane (**Figure 3g**), under a convex curvature of the midpiece (**Figure 3i**), or resting in a concave curvature (**Figure 3j**), and least common were those on the neck (not shown). Importantly, they increased in severity with dosage: for the high dosage group ERCs were larger and more proximally located at the neck in 16% of the sperm, versus 2% and 0% in the low dosage and control groups. Interestingly, sperm with all four types of ERCs uniformly retained the acrosomal cap (**Figure 3g–3i**) when analysis was performed on sperm stained to detect AR rates.

Frequencies of ERCs were similar for the control groups (8.8%–11.3%) for the three periods (**Table 2a**). At 24 h, while a 3×2 contingency table did not show a significant relationship of ERC rate and dosage ($\chi^2 = 2.19$; $P = 0.1389$), the 34% rate at the high dosage is highly significantly ($P < 0.001$) increased over the control (**Table 2a**). However, at 48 h (low [23.6%] and high [23.4%] dosages) and 120 h there was a highly significant relationship between ERC frequency and dosage ($\chi^2 = 17.17$, $P < 0.0001$), ($\chi^2 = 77.48$, $P < 0.0001$; **Table 2a**). Over time low dosage rates (5.9%–32.8%) showed a highly significant ($\chi^2 = 44.39$; $P < 0.0001$) increase of ERCs with exposure period (**Table 2a**), confirming that ATNP alters sperm maturation in the epididymis where ERCs are usually lost,²⁵ although they are also considered to be phagocytosed in the testis by Sertoli cells.²⁶

Correlation between the rates of excess residual cytoplasm and the inability of sperm to acrosome-react

To test for a correlation between ERC and inability to acrosome-react, induced sperm were re-analyzed and placed into one of four categories: presence/absence of ERC each with/without AR (**Table 2b**). A summary of data in **Table 2c** reveals that ERCs were seen in 16.2% of acrosome-reacted sperm compared to 83.8% of unreacted sperm, while none were seen in 46% and 54% of acrosome-reacted and unreacted sperm. The correlation between ERCs and the inability to

Table 1a: Rates of acrosome-reacted sperm after short-term exposure to ANTP

Postexposure periods (h)	Status	Number (%)		
		Control	Low dose	High dose
24	AR	270 (41.7) ^a	162 (38.6) ^b	152 (36.6) ^c
	No AR	377	255	263
	Total	647	417	415
48	AR	294 (69.5) ^{d,e}	361 (54.8) ^{d,f}	144 (36.3) ^{e,f}
	No AR	129	298	253
	Total	423	659	397
120	AR	339 (55.9) ^{g,h}	197 (30.6) ^g	190 (29.7) ^h
	No AR	267	441	449
	Total	606	638	639
Grand total	AR	903 (54.9) ^{i,j}	720 (42.0) ^{i,k}	486 (33.5) ^{j,k}
	No AR	773	994	965
	Total	1676	1714	1451

ATNP: anatase TiO₂ nanoparticles; AR: acrosome reaction; TiO₂: titanium dioxide. Identical letters refer to significant differences, using χ^2 analysis. ^aThe number is different from "a" and "b"; ^a $P < 0.001$: between control and low dose at 48 h; ^b $P < 0.001$: between control and high dose at 48 h; ^c $P < 0.001$: between low and high dose at 48 h; ^d $P < 0.001$: between control and low at 120 h; ^e $P < 0.001$: between control and high dose at 120 h; ^f $P < 0.001$: between grand control and low dose; ^g $P < 0.001$: between the grand control and high dose; ^h $P < 0.001$: between the grand low and high dose

Table 1b: Rates of motile sperm after short-term exposure to ANTP

Postexposure periods (h)	Status	Number (%)		
		Control	Low dose	High dose
24	Motile	283 (33.8) ^a	93 (8.4) ^a	401 (32.1)
	NM	554 (66.2)	1020 (91.6)	848 (67.9)
	Total	837	1113	1249
48	Motile	315 (21.2) ^b	268 (30)	91 (14.8) ^b
	NM	1166 (78.8)	626 (70)	524 (75.2)
	Total	1481	894	615
120	Motile	219 (20.9)	63 (15.7)	56 (14.1)
	NM	831 (79.1)	338 (84.3)	340 (85.9)
	Total	1050	401	396

ATNP: anatase TiO₂ nanoparticles; NM: nonmotile; TiO₂: titanium dioxide. Identical letters refer to significant differences, using χ^2 analysis. ^a $P < 0.001$: between motile control and low dose at 24 h; ^b $P < 0.001$: between motile control and high dose at 48 h

Table 2a: ERC rates after short-term exposure to ANTP

Postexposure periods (h)	Status	Number (%)		
		Control	Low dose	High dose
24	ERCs	81 (9.6) ^a	40 (5.9) ^y	267 (34.0) ^a
	No ERCs	761	638	518
	Total	842	678	785
48	ERCs	69 (11.3) ^{b,c}	178 (23.6) ^{b,y}	218 (23.4) ^c
	No ERCs	540	578	714
	Total	609	756	932
120	ERCs	80 (8.8) ^{d,e}	226 (32.8) ^{d,y}	275 (25.5) ^e
	No ERCs	826	463	803
	Total	906	689	1078

ERC: excess residual cytoplasm or cytoplasmic droplets; AR: acrosome reaction; ATNP: anatase TiO₂ nanoparticles; TiO₂: titanium dioxide. Identical letters refer to significant ($P < 0.001$) differences, using χ^2 analysis. ^a $P < 0.001$: control vs high dose at 24 h; ^b $P < 0.001$: control vs low dose at 48 h; ^c $P < 0.0001$: control vs high dose at 48 h; ^d $P < 0.0001$: difference in control vs low dose at 120 h; ^e $P < 0.0001$: control vs high dose at 120 h; ^y $P < 0.0001$: 24, 48, and 120 h at the low dose

acrosome-react was shown to be highly significant ($P < 0.001$) using the Cochran–Mantel–Haenszel test for repeated tests of independence with continuity correction.

Table 2b: Distribution of ERC and acrosome reaction rates after short-term exposure to ANTP

Postexposure periods (h)	Status	Number		
		Control	Low dose	High dose
24	ERC			
	AR	3	1	11
	No AR	7	14	58
	No ERC			
	AR	221	161	141
	No AR	171	241	205
	Total cells counted	402	417	415
48	ERC			
	AR	2	25	0
	No AR	9	10	16
	No ERC			
	AR	107	200	37
	No AR	88	192	144
	Total cells counted	206	427	197
120	ERC			
	AR	17	11	26
	No AR	41	157	191
	No ERC			
	AR	322	93	164
	No AR	226	171	258
	Total cells counted	606	432	639

ERC: excess residual cytoplasm or cytoplasmic droplets; AR: acrosome reaction; ANTP: anatase TiO₂ nanoparticles; TiO₂: titanium dioxide

Table 2c: Correlation of the rates ERC and the inability to acrosome-react after short-term exposure to ANTP

	Number (%)		Total
	AR	No AR	
ERC	96 (16.2)*	503 (83.8)*	599
No ERC	1446 (46.0)**	1696 (54.0)**	3142
Grand total	1542	2199	3741

ERC: excess residual cytoplasm or cytoplasmic droplets; ANTP: anatase TiO₂ nanoparticles; AR: acrosome reaction. **Cochran-Mantel-Haenszel test reveals a significant ($P < 0.001$) correlation between no ERC and AR

Reactive oxygen species and mitochondrial membrane potential levels (via Mitotracker) in sperm from treated males at 120 h postinjection

To determine the possible mechanism by which motility is lost after ANTP exposure, ROS was evaluated in sperm from 4 control and 3 treated males (high dose) 120 h postinjection. Flow cytometric analysis revealed that all treated animals had sperm with higher ROS levels than controls, as quantified by fluorescence intensity. **Figure 4a** shows significantly ($P < 0.00001$) increased fluorescence in treated versus untreated sperm, compared with the absence of the probe. For all samples, the average fluorescence units showed a > 2 -fold increase in sperm from the treated versus control, while the percentage of MitoTracker-negative cells (**Figure 4b**), reflecting a decrease in MMP, increased significantly ($P < 0.05$) in the treated group.

DISCUSSION

Our study shows, via TEM analysis, that ANTP deposited in the peritoneal cavity can travel to the scrotum where they aggregate in adipose tissues surrounding the testis and epididymis. This was seen in the short-term arm after 8 days postinjection of the high dose. That only one of 11 mice in this group displayed the aggregates is likely due to the inability to detect aggregates concealed in tissue folds. However, the detection of

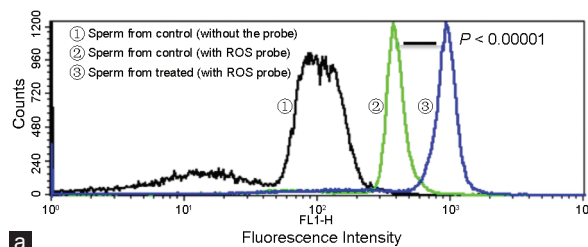
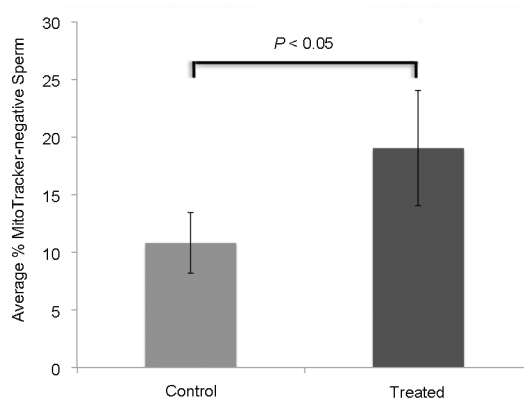
**a****b**

Figure 4: Increased reactive oxygen species (ROS) levels and decreased mitochondrial membrane potential (MMP) are seen in treated sperm, compared to controls. **(a)** Representative graph showing a significant ($P < 0.00001$) difference (> 2 -fold) in fluorescence intensities, as a function of ROS levels in control sperm and those treated with anatase titanium dioxide nanoparticles (ATNP) (high dose) at 120 h postinjection. In the absence of the detection probe the peak fluorescence units is 100. With 50 000 cells analyzed the mean fluorescence intensities were compared in a *t*-test. **(b)** Sperm stained with MitoTracker mitochondrial Red CMXRos probe were analyzed to detect unstained negative cells, reflecting depolarization of the mitochondrial membrane and decreased MMP which accompanies increased ROS generation. A *t*-test showed significantly ($P < 0.05$) more Mitotracker negative sperm in ATNP-treated males than in controls. 5×10^4 sperm were analyzed for each of the three animals in the two groups.

aggregates at a site distinct from the entry point indicates that ANTP travel to the scrotum where they bioaccumulate, similar to bulk metals.²⁷ Our observation is consistent with the report that nanoparticles are capable of self-aggregation *in vivo*²⁸ and supports studies reporting that TNP are capable of entering the systemic circulation and relocating.^{29,30}

Histological analysis showed that the interstitial spaces in the testes of treated animals were enlarged after the longest period in the short-term and after up to 3 weeks in the long-term arm. At these times some of the seminiferous tubules appeared disorganized with a paucity of germ cells, corroborating the report that TNP may be endocrine disruptors.³¹ Our finding of enlarged interstitial spaces with significantly increased numbers of apoptotic cells is in line with a report indicating that NP escape the blood-testis barrier and are likely to be located in the intercellular space^{5,32} where they may cause inflammation.^{6,32} Indeed evidence for an inflammatory response was detected in epididymal tissues and ELF of treated animals: there was both increased and decreased cytokine expression. (The latter may have occurred to prevent autoimmune response to sperm). Accompanying inflammation was a significant increase in germ cell apoptosis. This confirms earlier studies using larger doses of nondefined TNP^{12,16} and indicates the highly reactive nature of the anatase polymorph⁸ used in the present study in much smaller doses (2.5 – 5 mg kg⁻¹ BW).

With respect to sperm morphology and function after ATNP treatment, the long-term and short-term arms gave different results. For the long-term, there were no significant differences between treated and controls for structural or functional characteristics. Since differences were detected in the short-term arm, our results suggest that the effects are transient, and are due to inflammation which resolves over time. It is possible that in the long-term arm affected sperm would have already passed through the epididymis at the time of analysis, consistent, with the possibility of the reversal of the effects of NP over time.⁵

In the short-term arm, starting from the first day of injection, epididymal sperm were exposed to ATNP for total periods of 4, 5, or 8 days, fractions of the 14–19 days that sperm from ICR mice were shown to reside in the epididymis.³³ During this period they undergo maturational changes via the luminal environment. The finding of highly significant increases in flagellar abnormalities after ATNP exposure suggests that ATNP enter and alter the epididymal luminal environment, as evidenced by changes in the cytokine status. Although the epididymis is protected by the blood-epididymis barrier,³⁴ nanoparticles have demonstrated their ability to traverse biological barriers, particularly the blood-brain barrier.^{7,13,35,36}

Since bioaccumulation of metallic compounds in the scrotum induces its effects by ROS,²⁷ we asked if the reduction of hyperactivated motility resulting from short-term exposure is accompanied by elevated levels of ROS and reduced MMP. We detected > 2-fold increases of ROS and increased percent of MitoTracker–negative cells in treated versus controls, showing the expected inverse relationship between ROS and MMP. Elevated ROS levels are known to cause peroxidative damage to sperm plasma membranes,^{27,37} a key mechanism for motility loss.³⁸ They are also associated with decreased AR rates,³⁹ increased frequencies of ERC^{25,40} and flagellar abnormalities, all of which showed dose-response relationships in this study. At 48 h and 120 h exposures there were significant relationships between ERC frequency and the dosage of ATNP. Additionally, the size and severity of the ERC increased with dosage. The high dosage showed the highest proportion of ERC at the neck, a location indicative of failure of normal epididymal maturation with resulting infertility.⁴⁰ Interestingly, we detected a significant correlation between ERC frequency and unreacted acrosomes. This correlation suggests a novel mechanism for the infertility of sperm with ERCs. Reports that ERC in human sperm is associated with infertility^{27,40} suggest that ATNP exposure in doses comparable to those used in the present study may have a deleterious effect on human fertility via increased ERC frequency and reduced motility. Both of these are likely to be mediated by elevated ROS levels, as is the DNA damage detected by the TUNEL assay.

CONCLUSIONS

Our study clearly indicates that ATNP bioaccumulate in the scrotum where they self-aggregate and lead to testicular histopathology, while severely affecting epididymal sperm maturation and function, after 4–8 days, but not 10 days to 5 weeks, postinjection. Frequencies of flagellar abnormalities, inability to acrosome-react, ERCs, and reduced motility were elevated and accompanied by increased ROS levels in sperm of treated males. Further studies are required to determine whether sperm fertilizing ability *in vivo/in vitro* is affected by ATNP. Since TNP has been shown to induce photogenotoxic events in human sperm exposed *in vitro*,⁴¹ our study points to a potential source of sperm defects which are known to have detrimental effects on human fertility.

AUTHOR CONTRIBUTIONS

SIS synthesized the ANTP and MAS and RM administered the injections and performed most of the experiments. RGA prepared

the material for histology and interpreted the H and E slides. SD performed the hyperactivated motility assays. DSG performed the flow cytometric assays and assisted with the interpretation of the data. PAMD performed the assays for the ROS, the MMP and the apoptotic assays, designed and coordinated the project.

COMPETING INTERESTS

The authors declare that they have no competing interests.

ACKNOWLEDGEMENTS

The work was supported by an EPSCOR Seed Grant to Syed I Shah and Patricia A Martin-DeLeon and 5P20RR015588 and NIH-1R03 HD073523-01A1 to Patricia A Martin-DeLeon. We are grateful to Dr. John McDonald for assistance with statistics and Amal Al-Dossary for help with sectioning, confocal analysis of the apoptotic cells, and the graphics.

REFERENCES

- 1 Kaida T, Kobayashi K, Adachi M, Suzuki F. Optical characteristics of titanium oxide interference film and the film laminated with oxides and their applications for cosmetics. *J Cosmet Sci* 2004; 55: 219–20.
- 2 Wang W, Gu B, Liang L, Hamilton WA, Wesolowski DJ. Synthesis of Rutile α -TiO₂ nanocrystals with controlled size and shape by low-temperature hydrolysis: effects of solvent composition. *J Phys Chem B* 2004; 108: 14789–92.
- 3 Mills A, Elliott N, Hill G, Fallis D, Durrant JR, *et al*. Preparation and characterisation of novel thick sol-gel titania film photocatalyst. *Photochem Photobiol Sci*. 2003; 5:591-6.
- 4 Modestov AD, Lev O. Photocatalytic oxidation of 2,4-dichlorophenoxyacetic acid with titania photocatalyst: comparison of supported and suspended TiO₂. *J Photochem Photobiol A* 1998; 112: 261–70.
- 5 Hougaard KS, Campagnolo L. Reproductive toxicity of engineered nanoparticles. In: Fadeel B, Pietroiusti A, Shvedova AA, editors. *Adverse Effects of Engineered Nanoparticles*. San Diego, U.S.A, Academic Press: Elsevier; 2012. p. 225–48.
- 6 Iavicoli I, Leso V, Bergamaschi A. Toxicological effects of titanium dioxide nanoparticles: a review of *in vivo* studies. *J Nanomater* 2012; 36: 1–36.
- 7 Ema M, Kobayashi N, Naya M, Hanai S, Nakanishi J. Reproductive and developmental toxicity studies of manufactured nanomaterials. *Reprod Toxicol* 2010; 30: 343–52.
- 8 Sayes CM, Wahi R, Kurian PA, Liu Y, West JL, *et al*. Correlating nanoscale titania structure with toxicity: a cytotoxicity and inflammatory response study with human dermal fibroblasts and human lung epithelial cells. *Toxicol Sci* 2006; 92: 174–85.
- 9 Barnes PJ. Reactive oxygen species and airway inflammation. *Free Radic Biol Med* 1990; 9: 235–43.
- 10 Cho M, Chung H, Choi W, Yoon J. Linear correlation between inactivation of *E. coli* and OH radical concentration in TiO₂ photocatalytic disinfection. *Water Res* 2004; 38: 1069–77.
- 11 Maness PC, Smolinski S, Blake DM, Huang Z, Wolfrum EJ, *et al*. Bactericidal activity of photocatalytic TiO (2) reaction: toward an understanding of its killing mechanism. *Appl Environ Microbiol* 1999; 65: 4094–8.
- 12 Sycheva LP, Zhurkov VS, Iurchenko VV, Dauge-Dauge NO, Kovalenko MA, *et al*. Investigation of genotoxic and cytotoxic effects of micro- and nanosized titanium dioxide in six organs of mice *in vivo*. *Mutat Res* 2011; 726: 8–14.
- 13 Takeda K, Suzuki KI, Ishihara A, Kubo-Irie M, Fujimoto R, *et al*. Nanoparticles transferred from pregnant mice to their offspring can damage the genital and cranial nerve systems. *J Health Sci* 2009; 55: 95–102.
- 14 Komatsu T, Tabata M, Kubo-Irie M, Shimizu T, Suzuki K, *et al*. The effects of nanoparticles on mouse testis Leydig cells *in vitro*. *Toxicol in vitro* 2008; 22: 1825–31.
- 15 Asare N, Instanes C, Sandberg WJ, Refsnes M, Schwarze P, *et al*. Cytotoxic and genotoxic effects of silver nanoparticles in testicular cells. *Toxicology* 2012; 291: 65–72.
- 16 Guo LL, Liu XH, Qin DX, Gao L, Zhang HM, *et al*. Effects of nanosized titanium dioxide on the reproductive system of male mice. *Zhonghua Nan Ke Xue* 2009; 15: 517–22.
- 17 Oakberg EF. Duration of spermatogenesis in the mouse and timing of stages of the cycle of the seminiferous epithelium. *Am J Anat* 1956; 99: 507–16.
- 18 Robaire B, Hinton BT, Orgebin-Crist M. The epididymis. In: Neill J, Plant T, Pfaff D, Challis J, Kretser D, editors. *Knobil and Neill's Physiology of Reproduction*. New York: Raven Press; 2006. p. 1071–1148.
- 19 Buzby S, Barakat MA, Lin H, Ni C, Rykov SA, *et al*. Visible light photocatalysis with nitrogen doped anatase titanium dioxide nanoparticles prepared by plasma assisted chemical vapor deposition. *J Vac Sci Technol* 2006; B 24: 1210–4.
- 20 Zhang H, Martin-DeLeon PA. Mouse epididymal Spam1 (PH-20) is released *in vivo* and *in vitro*, and Spam1 is differentially regulated in testis and epididymis. *Biol Reprod* 2001; 65: 1586–93.
- 21 Moller CC, Bleil JD, Kinloch RA, Wassarman PM. Structural and functional

- relationships between mouse and hamster zona pellucida glycoproteins. *Dev Biol* 1990; 137: 276–86.
- 22 Morales CR, Badran H, El-Alfy M, Men H, Zhang H, *et al*. Cytoplasmic localization during testicular biogenesis of the murine mRNA for Spam1 (PH-20), a protein involved in acrosomal exocytosis. *Mol Reprod Dev* 2004; 69: 475–82.
- 23 Setsukinai K, Urano Y, Kakinuma K, Majima HJ, Nagano T. Development of novel fluorescence probes that can reliably detect reactive oxygen species and distinguish specific species. *J Biol Chem* 2003; 278: 3170–5.
- 24 Wang MJ, Ou JX, Chen GW, Wu JP, Shi HJ, *et al*. Does prohibitin expression regulate sperm mitochondrial membrane potential, sperm motility, and male fertility? *Antioxid Redox Signal* 2012; 17: 513–9.
- 25 Clermont Y. Kinetics of spermatogenesis in mammals: seminiferous epithelium cycle and spermatogonial renewal. *Physiol Rev* 1972; 52: 198–236.
- 26 Cooper TG. Cytoplasmic droplets: the good, the bad or just confusing? *Hum Reprod* 2005; 20: 9–11.
- 27 Doreswamy K, Shrilatha B, Rajeshkumar T, Muralidhara. Nickel-induced oxidative stress in testis of mice: evidence of DNA damage and genotoxic effects. *J Androl* 2004; 25: 996–1003.
- 28 Baveye P, Laba M. Aggregation and toxicology of titanium dioxide nanoparticles. *Environ Health Perspect* 2008; 116: A152.
- 29 Kreyling WG, Semmler M, Erbe F, Mayer P, Takenaka S, *et al*. Translocation of ultrafine insoluble iridium particles from lung epithelium to extrapulmonary organs is size dependent but very low. *J Toxicol Environ Health A* 2002; 65: 1513–30.
- 30 Takenaka S, Karg E, Roth C, Schulz H, Ziesenis A, *et al*. Pulmonary and systemic distribution of inhaled ultrafine silver particles in rats. *Environ Health Perspect* 2001; 109 Suppl 4: 547–51.
- 31 Iavicoli I, Fontana L, Leso V, Bergamaschi A. The effects of nanomaterials as endocrine disruptors. *Int J Mol Sci* 2013; 14: 16732–801.
- 32 Joshi SC, Kaushik U. Nanoparticles and reproductive toxicity: an overview. *Res J Pharm Biol Chem Sci* 2013; 4: 1396–1410.
- 33 Martin-DeLeon PA, Boice ML. Sperm aging in the male and cytogenetic anomalies. An animal model. *Hum Genet* 1982; 62: 70–7.
- 34 Hoffer AP, Hinton BT. Morphological evidence for a blood-epididymis barrier and the effects of gossypol on its integrity. *Biol Reprod* 1984; 30: 991–1004.
- 35 Lockman PR, Koziara JM, Mumper RJ, Allen DD. Nanoparticle surface charges alter blood-brain barrier integrity and permeability. *J Drug Target* 2004; 12: 635–41.
- 36 Long TC, Tajuba J, Sama P, Saleh N, Swartz C, *et al*. Nanosize titanium dioxide stimulates reactive oxygen species in brain microglia and damages neurons *in vitro*. *Environ Health Perspect* 2007; 115: 1631–7.
- 37 Baker MA, Aitken RJ. Reactive oxygen species in spermatozoa: methods for monitoring and significance for the origins of genetic disease and infertility. *Reprod Biol Endocrinol* 2005; 3: 67.
- 38 Baumber J, Ball BA, Gravance CG, Medina V, Davies-Morel MC. The effect of reactive oxygen species on equine sperm motility, viability, acrosomal integrity, mitochondrial membrane potential, and membrane lipid peroxidation. *J Androl* 2000; 21: 895–902.
- 39 Ichikawa T, Oeda T, Ohmori H, Schill WB. Reactive oxygen species influence the acrosome reaction but not acrosin activity in human spermatozoa. *Int J Androl* 1999; 22: 37–42.
- 40 Aziz N, Saleh RA, Sharma RK, Lewis-Jones I, Esfandiari N, *et al*. Novel association between sperm reactive oxygen species production, sperm morphological defects, and the sperm deformity index. *Fertil Steril* 2004; 81: 349–54.
- 41 Gopalan R, Osman I, Amani A, de Matas M, Anderson D. The effect of zinc oxide and titanium dioxide nanoparticles in the comet assay with UVA photoactivation of human sperm and lymphocytes. *Nanotoxicology* 2009; 3: 33–9.